# Fluorescence Spectra of Phenanthridine Isolated in the Supersonic Jet Expansion — An *Ab Initio* Analysis

I. Deperasińska[a,*], J. Prochorow[a] and Y. Stepanenko[b]

[a]Institute of Physics, Polish Academy of Sciences
al. Lotników 32/46, 02-668 Warsaw, Poland

[b]Institute of Physical Chemistry and The Laser Center
Polish Academy of Sciences, Kasprzaka 44, 01-224 Warsaw, Poland

Following the analysis of laser induced fluorescence spectrum of 7,8-benzoquinoline molecule, observed under conditions of isolation in the supersonic jet expansion, the *ab initio* analysis of laser induced fluorescence spectrum of phenanthridine, observed under the same experimental conditions, was performed. This analysis included: optimization of equilibrium geometry of phenanthridine in its first excited $S_1$ singlet state and computations of the frequencies of vibrational fundamental modes together with their geometry changes between the excited and the ground state. Comparison of the results of calculations with experimental data revealed their good agreement and an increase in the vibrational activity in the fluorescence spectrum in comparison to fluorescence spectrum of phenanthrene molecule (which is a parent aromatic hydrocarbon of phenanthridine and of 7,8-benzoquinoline). Such an increase in vibrational activity in the fluorescence spectrum was earlier observed also for 7,8-benzoquinoline molecule. Present analysis shows that this effect is due to molecular symmetry reduction caused by the substitution of nitrogen atom into the aromatic rings system of phenanthrene, as well as to the changes of equilibrium structure between the ground and excited states.

PACS numbers: 82.20.Wt, 31.15.Ar, 33.20.Tp

## 1. Introduction

The prime effect of the replacement of one C–H group in polycyclic aromatic hydrocarbon (PAH) molecule by a single nitrogen (N) atom (and thus formation of monoazaderivative of PAH) is a creation of excited states which belong to the $(n, \pi^*)$ electronic configuration. It is well known that the appearance of the $(n, \pi^*)$

*corresponding author; e-mail: deper@ifpan.edu.pl

electronic states (in both, the singlet and triplet manifolds) may deliver new paths for radiative and nonradiative decays of different excited N-heterocyclic aromatic hydrocarbon molecules (due to the mixing and coupling between $(\pi, \pi^*)$ and $(n, \pi^*)$ electronic configurations, see for instance [1, 2]).

Furthermore, non-bonding $n$-electrons of N atom are vulnerable to specific interactions with the molecules of the surroundings, and this may lead, in protic solvents, to the hydrogen-bond formation or protonation. Hence, in some cases fluorescence and/or phosphorescence of N-heterocyclic aromatic hydrocarbons are extremely sensitive to the solvent. In the case of monoazaderivatives of tricyclic aromatic hydrocarbons (such as anthracene and phenanthrene) solvent-sensitivity of fluorescence seems to be related to the relative energetics of $^1(\pi, \pi^*)$ and $^1(n, \pi^*)$ excited singlet states in a particular molecule under consideration, as well as to the capability of non-bonding $n$-electrons to the formation of the hydrogen bonds [3–5].

Recently we have reported observations of the laser-induced single-vibronic level (SVL) fluorescence spectra of two monoazaderivatives of phenanthrene (PH) — phenanthridine (PHN) and 7,8-benzoquinoline (BQ) — monitored under conditions of jet-cooling in a supersonic expansion of helium. Contrary to the experiments in condensed phases (in liquid solutions, especially) such conditions of isolation of excited molecules, in collision-free expansion, have revealed rather distinct differences between the fluorescence excitation (absorption) and fluorescence spectra of both molecules under study [6]. In a subsequent paper, the results of an *ab initio* analysis of the vibrational structure of observed fluorescence spectrum of BQ has been presented [7]. The results of this analysis have been compared with the results of analysis of similar observations of jet-cooled fluorescence spectra for the PH molecule [8] — parent aromatic hydrocarbon for both monoazaphenanthrenes under consideration. This comparison has led to the conclusions that the fluorescence spectra originating from excited $S_1$ singlet state (which is an electronic $(\pi, \pi^*)$ state) of BQ molecule can be rationalized in terms of reduction of molecular symmetry in BQ caused by the substitution of N atom into the aromatic rings system of PH molecule.

This paper is a second part of our studies of *ab initio* analysis of fluorescence spectra of molecules of monoazaphenanthrenes, observed under conditions of isolation in the supersonic molecular beam. We perform here an *ab initio* analysis of the fluorescence spectrum of PHN, following all the steps outlined in the first paper of this series in which such an analysis of the fluorescence spectrum of 7,8-benzoquinoline has been reported [7]. Hence, in order to avoid the repetition of the details of the employed procedures of analysis, we ask the Reader to draw his attention to our earlier papers [7] and [9], in which procedures used for optimization of excited- and ground-state equilibrium structures, and for computations of their molecular parameters and vibronic transitions are described and the results of different optimization and computational methods are compared. We note that all the calculations have been performed with the GAUSSIAN 98 programs [10].

## 2. Geometry and electronic structure of the ground and excited singlet states of phenanthridine

It was found earlier that the lengths of chemical bonds, in the ground state of PHN molecule, differ from the lengths of relevant bonds in PH molecule. The largest changes, caused by the substitution of an N atom into the PH molecule (equivalent to the change of PH molecule into PHN molecule), are those in the central ring, where N atom replaces C–H bond. Changes of the bond lengths, accompanied by the changes of the angles between relevant adjacent bonds in PHN molecule, and the net result of these changes is the deformation of aromatic rings system of parent aromatic hydrocarbon (PH) [9]. Quite similarly, in the case of BQ molecule the deformation of the ground state geometry is the largest in the external ring, where the N atom is located. However, it should be noticed that the changes of bond lengths in both monoazaphenanthrenes are not confined to the aromatic ring in which N atom resides, but extend over the entire aromatic rings system. The relatively high symmetry of the ground-state phenanthrene molecule (point group $C_{2v}$) is broken in its monoazaderivatives.

Figure 1 illustrates the differences between the optimized equilibrium geometry of the ground ($S_0$) and excited ($S_1$) singlet states of PHN molecule. The numbers (in bold) indicate the changes of the bond lengths upon electronic transition from $S_0$ and $S_1$ excited state (in both states molecule remains planar), as obtained within the RHF/6-31G(d) and RCIS/6-31G(d) methods, respectively (verified by the calculations of the vibrational frequencies, which showed that the true minima were obtained). It is seen that upon excitation of PHN molecule to $S_1$ state, the lengths of bonds in the central ring are subject to the largest changes, and clearly they are much smaller in the peripheral aromatic rings. On the other hand, comparison of the corresponding changes of the lengths of bonds upon excitation of phenanthrene molecule from the ground to the excited $S_1$ state (see Fig. 1 in [7]) shows that in both molecules electronic transition is delocalized over entire aromatic rings system in a very similar manner.
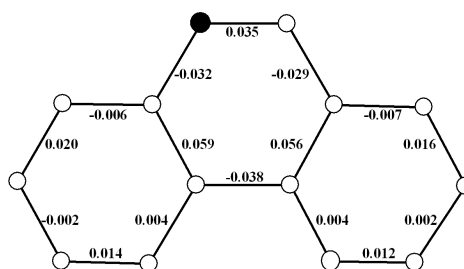


Fig. 1. Optimized equilibrium geometry of the excited $S_1$ singlet state of phenanthridine molecule (position of nitrogen atom is marked by the black dot). The change of the length (in Å) of a given bond, relatively to its length in the $S_0$ ground state, is given by bold numbers.

The energies of electronic transitions from the ground to the excited states (of RCIS/6-31G(d) optimized geometry) for PHN molecule, computed by the time dependent density functional theory (TD DFT) method at B3LYP/6-31G(d) level, have located its first excited singlet state at 31464 cm$^{-1}$ (and with the oscillator strength of $f = 0.007$). This is the $^1(\pi, \pi^*)$ electronic state and its energy is reasonably close to experimental transition of 29391 cm$^{-1}$ observed in the supersonic jet (see next section). The difference of 2073 cm$^{-1}$ between the calculated and experimental energy of the first excited $S_1$ singlet state can be considered as a quite satisfactory test for the computational methods employed in this study.

The second excited singlet state ($S_2$) with energy of 33496 cm$^{-1}$ is identified as $^1(n, \pi^*)$ state. The energy gap between the first excited $^1(\pi, \pi^*)$ and the $^1(n, \pi^*)$ state in PHN (i.e. $S_2 - S_1$ separation) equals to 2032 cm$^{-1}$. Thus, it amounts to less than half of the corresponding value of the separation between the first excited $^1(\pi, \pi^*)$ and $^1(n, \pi^*)$ states found for BQ molecule. We recall, however, that in the case of BQ, $^1(n, \pi^*)$ state is the third excited ($S_3$) state in the singlets manifold (located at the energy of 35053 cm$^{-1}$, while the energy of $S_1$ $^1(\pi, \pi^*)$ singlet state is 30920 cm$^{-1}$ [9]).

## 3. Analysis of the fluorescence spectrum of jet-cooled PHN molecules

In order to carry out the analysis of the vibrational (vibronic) structure of the fluorescence spectrum one has to determine the displacement parameters ($\Delta$) for each particular vibrational mode under consideration. With the assumption that the identity of the normal modes is preserved in $S_1 \rightarrow S_0$ transitions, the displacement parameters ($\Delta$) are calculated as a projection of the geometry change between the excited and ground state onto the vectors of normal modes of the ground state [11]. The accuracy of the determination of any particular vibrational frequency in the spectrum, is a prime condition of the reliability of the analysis of the vibrational structure. This in turn calls for the high resolution of vibrational structure of recorded fluorescence spectra. In the present case such condition is secured (to some extent) by the fact that the analysis is carried out for the experimental data which were gathered under conditions of supersonic jet expansion [6].

### 3.1. Summary of experimental data

Figure 2 illustrates results of observations of the laser induced fluorescence (LIF) excitation spectra and dispersed fluorescence spectra of PHN molecules, monitored under conditions of jet-cooling supersonic expansion. LIF excitation spectra, shown in Fig. 2, were recorded for total fluorescence, with the resolution limited by the spectral width of the laser exciting line, while resolution of the dispersed fluorescence spectra was limited by the spectral width of the dispersing apparatus (cf. also Fig. 2 and Fig. 3 of Ref. [6], respectively). It is very instructive to see how rich and sharp is the vibrational structure of the LIF excitation spectrum in the whole monitored spectral region in comparison to that recorded in the fluorescence spectrum.
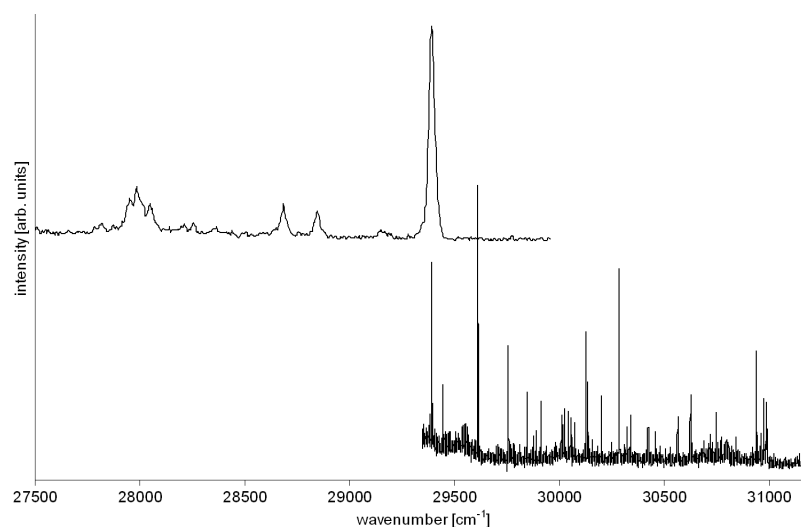
Fig. 2. Excitation spectrum of laser induced fluorescence (*bottom-right*) and dispersed fluorescence spectrum (*top-left*) of phenanthridine molecules isolated in the supersonic jet expansion of helium (compiled after [6]). The energy of electronic vibrationless origin transition in both spectra is 29391 cm$^{-1}$. Intensity scales of excitation and fluorescence spectra are not related one to each other (they illustrate only relative intensity distribution within each spectrum).

The (0,0) origin band of LIF excitation spectrum of PHN is located at 29391 cm$^{-1}$, and is shifted by 63 cm$^{-1}$ toward higher energies (a blue shift) relative to the position of the (0,0) origin band in the LIF excitation spectrum of its parent aromatic hydrocarbon, phenanthrene, observed under jet-cooling conditions. This is a shift direction opposite than that observed in the case of BQ molecule, in which the (0,0) origin band of LIF excitation spectrum displays a red shift (toward lower energies) of 102 cm$^{-1}$ relative to PH molecule [6, 8].

Dispersed fluorescence spectrum of PHN excited in its (0,0) origin is very weak (in part, due to the fact that most of its intensity is carried out by the resonant 0–0 radiative transition), and for this reason vibrational structure of the fluorescence spectrum is diffused. In addition, in some regions (e.g. 1200–1400 cm$^{-1}$ from the origin transition), an overlap of several vibronic transitions leads to the blurring of the structure of observed fluorescence spectrum. For these reasons, the number of vibronic transitions, frequency of which can be identified with a high precision, is limited. Hence, as in the case of the previous analysis of fluorescence of BQ molecule, also the present analysis of the vibrational structure of PHN fluorescence was performed for SVL fluorescence spectrum, i.e. fluorescence spectrum observed as a result of excitation to the selected vibronic level, with energy higher than the 0–0 energy for the ground-to-first excited ($S_0 \rightarrow S_1$) transition.

### 3.2. Analysis of the vibrational structure of the SVL fluorescence spectrum of phenanthridine

As can be seen in Fig. 2, the most intense vibronic transition in the LIF excitation spectrum of PHN molecules is that which terminates at the level with energy of 220 cm$^{-1}$ above the origin transition (cf. also Fig. 2 in [6]).

When the excitation is tuned to the energy of this vibrational level (i.e.: $29391 + 220 = 29611$ cm$^{-1}$), the SVL fluorescence spectrum, shown in Fig. 3, is observed. Quite clearly, in this spectrum vibrational bands become more intense
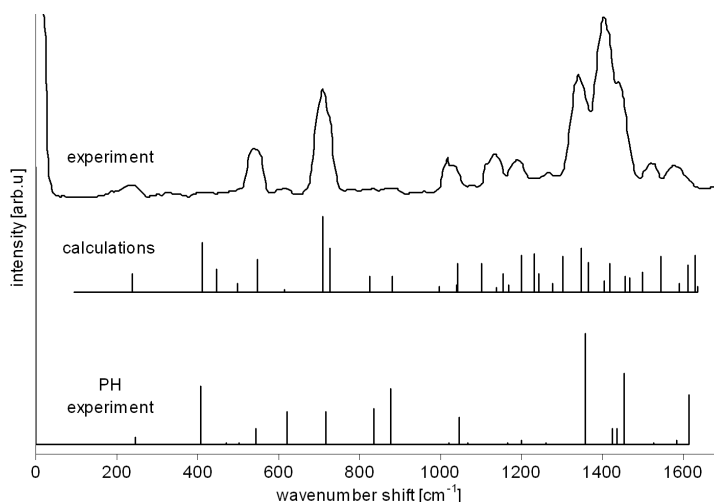


Fig. 3. (*Top*) Single vibronic level fluorescence spectrum of phenanthridine observed after excitation with excess energy of 220 cm$^{-1}$ above the origin transition (excitation energy $29391 + 220 = 29611$ cm$^{-1}$). (*Middle*) Calculated vibrational frequencies of the fluorescence spectrum. The heights of sticks correspond to the magnitude of $\Delta$ (for details see text and Table I). (*Bottom*) Dispersed fluorescence spectrum of jet-cooled PH molecule. The heights of sticks correspond to relative intensity distribution within the spectrum (compiled after data of [8]). All spectra are displayed as the energy shifts relative to the energy of the origin transition.

as compared to the spectrum excited in the origin band (cf. Fig. 5 in [6]). However, contrary to the observations of SVL fluorescence spectra of BQ molecule (cf. Fig. 4 in [6] and Fig. 3 in [7]) some vibrational bands become wider, and this results in the loss of structure and in the increased uncertainty of determination of vibrational frequencies. On top of that, Fig. 3 clearly demonstrates that observed SVL fluorescence spectrum has a rich background, which may contain underneath a number of some low-intensity vibrations.

The frequencies of some vibrational bands observed in the SVL fluorescence spectrum (given in Fig. 3), which are determined with accuracy better than

TABLE I

Calculated vibrational frequencies ($\nu$) for $S_1 \rightarrow S_0$ electronic transition (with corresponding displacement parameter $\Delta$ of each vibrational mode) and vibrational experimental frequencies observed in the fluorescence spectrum from single vibronic level of phenanthridine isolated in jet-cooled supersonic expansion. For comparison, ground--state vibrational frequencies observed in IR spectrum of phenanthridine isolated in low-temperature Ar matrix [12] are also given.

| Calculations | | Experiment | IR | Calculations | | Experiment | IR |
|---|---|---|---|---|---|---|---|
| $\nu$ [cm$^{-1}$] | $\Delta$ | $\nu$ [cm$^{-1}$] | $\nu$ [cm$^{-1}$] | $\nu$ [cm$^{-1}$] | $\Delta$ | $\nu$ [cm$^{-1}$] | $\nu$ [cm$^{-1}$] |
| 237 | 0.008 | 235 | | 1198 | 0.016 | 1192 | 1195 |
| 410 | 0.022 | 412* | | 1229 | 0.017 | | 1228 |
| 444 | 0.010 | | 449 | 1243 | 0.008 | | 1241 |
| 499 | 0.003 | | | 1276 | 0.004 | } 1271 | |
| 546 | 0.014 | 542 | | 1299 | 0.015 | | 1297 |
| 615 | 0.001 | 623* | 616 | 1346 | 0.019 | } 1341 | |
| 708 | 0.033 | } 709 | 713 | 1363 | 0.013 | | 1347 |
| 724 | 0.019 | | 728 | 1401 | 0.005 | } 1404 | 1400 |
| 825 | 0.007 | 843* | | 1417 | 0.012 | | 1419 |
| 880 | 0.007 | 893* | 890 | 1456 | 0.007 | } 1441 | 1453 |
| 997 | 0.003 | | 1006 | 1467 | 0.006 | | 1464 |
| 1037 | 0.003 | } 1015 | 1040 | 1498 | 0.008 | } 1520 | 1493 |
| 1040 | 0.012 | | 1042 | 1542 | 0.015 | | 1531 |
| 1102 | 0.012 | | 1103 | 1587 | 0.004 | } 1580 | 1580 |
| 1136 | 0.002 | } 1132 | 1138 | 1609 | 0.012 | | 1596 |
| 1152 | 0.008 | | 1146 | 1626 | 0.016 | | 1625 |
| 1166 | 0.003 | | 1166 | 1635 | 0.002 | | 1642 |

$\pm 5$ cm$^{-1}$, are collected in Table I, which also lists the computed (RHF/6-31G$^{**}$) frequencies of the fundamental vibrations of the ground state expected in the $S_1 \rightarrow S_0$ transition. Those vibrations are all of $a'$ symmetry and are characterized by the different equilibrium position in the excited and in the ground state (i.e. by the displacement parameter $\Delta \neq 0$, as seen in Table I). The results of computations are also presented in the form of a stick diagram in Fig. 3.

The comparison of calculated and experimental data of Table I shows that exact coincidence between those two sets of data is rather poor, but the deviations are in some cases very small (e.g. 235 and 237 cm$^{-1}$, 708 and 709 cm$^{-1}$) or moderate (e.g. 546 and 542 cm$^{-1}$, 1198 and 1192 cm$^{-1}$, 1346 and 1341 cm$^{-1}$, or 1587 and 1580 cm$^{-1}$) and are within the experimental error limits (set by a final resolution of $\approx 40$ cm$^{-1}$ in the SVL fluorescence spectrum [6]). However, in some spectral regions, a precise assignment of observed and calculated frequencies is a rather difficult task, due to either low intensity of observed vibrational bands (marked by asterisks in Table I), or to the "crowd" of vibrational transitions in calculated spectrum, which, as seen in Fig. 3, may appear in the experimental

spectrum as wide bands of several overlapping (close-lying) transitions (in Table I such transitions are indicated by the brackets). It is evident, however, that although vibrational structure of experimental fluorescence spectrum of PHN is not well resolved, its overall envelope follows and reflects calculated vibrational structure.

Vibronic transitions from excited $S_1$ state to the ground $S_0$ state are by virtue probing vibrational structure of the ground state and thus the ground-state IR spectra can be used as an additional comparative test in the vibrational analysis of the experimental fluorescence spectrum. With this in mind the investigations of the mid-infrared ground-state spectra of PHN molecules isolated in low-temperature inert matrix of Ar at 15 K have been carried out in this lab (the spectral data together with the results of normal mode analysis of this IR spectrum will be published elsewhere [12]). The numerical results of these investigations are given in Table I. It is seen that the observed ground-state IR spectrum (in the accessible region above 400 cm$^{-1}$) contains much more vibrational features than the SVL fluorescence spectrum. This is not surprising, as the vibrational activity of a given mode in the fluorescence spectrum is controlled by the change of its equilibrium position geometry between the excited and ground state (i.e. by a non-zero displacement parameter $\Delta$). This is also reflected by the comparison of IR spectrum with the calculated vibronic structure of SVL fluorescence spectrum, which shows that some of the calculated frequencies of fluorescence spectrum do not have their counterparts in the ground-state IR spectrum. However, those observed in the IR spectrum well coincide with the computed vibrational frequencies of the fluorescence spectrum. Thus, in our opinion, the results of comparison of the ground-IR spectrum with SVL fluorescence spectrum of PHN positively verifies applied methods of analysis of these latter.

As in the case of analysis of the fluorescence spectrum of BQ, we should compare the spectrum of PHN with fluorescence spectrum of its parent aromatic hydrocarbon molecule, i.e. with the fluorescence spectrum of phenanthrene observed from the supersonic jet expansion [8]. This spectrum is also given in Fig. 3 (and tabulated in Table II), and even at first glance it is clear that its vibrational structure is relatively poor in comparison with the calculated structure of the fluorescence spectrum of PHN molecule, or in other words, it is clear that the number of vibrations active in PHN spectrum was increased compared to PH spectrum. If we refer to the data gathered earlier for the fluorescence spectrum of BQ, observed under conditions of supersonic molecular beam isolation [6, 7], then it becomes obvious that the fluorescence spectra of all three molecules under consideration exhibit clear differences, especially noticeable from the point of view of their vibronic structure (vibrational activity), which increases in order: PH $\rightarrow$ PHN $\rightarrow$ BQ.

The same arguments, as used earlier in the discussion of the relation between calculated and experimental data of PHN fluorescence, also hold true for the com-

parison between PHN and PH fluorescence spectra. For instance, vibrational band at 709 cm$^{-1}$ in the observed fluorescence spectrum of PHN, which could be related to 714 cm$^{-1}$ band in PH spectrum, may be in fact due to calculated 708 and 724 cm$^{-1}$ vibrations, which are also observed in ground-state IR spectrum of PHN (cf. Table I). Similarly, very intense band centred at $\approx 1400$ cm$^{-1}$ and with drastically changed relative intensity distribution (as compared to that seen in PH spectrum) can be built up with participation even of six fundamental frequencies (in Table I, calculated frequencies from the range 1363–1467 cm$^{-1}$). Such an overlap (and/or mixing) of vibrational modes may result in a rather poor agreement between the observed and calculated intensities of fundamental transitions [13].

TABLE II

Vibrational frequencies observed in dispersed fluorescence spectra of jet-cooled phenantridine (PHN; this work and [6]), 7,8-benzoquinoline (BQ; after [6, 7]) and phenanthrene (PH; after [8]).

| PHN, $\nu$ [cm$^{-1}$] | BQ, $\nu$ [cm$^{-1}$] | PH, $\nu$ [cm$^{-1}$] |
|---|---|---|
| 235 | 247* | 248 |
| 412* | 410 | 408 |
| | 467 | 471 |
| 542 | 557 | 544 |
| 623* | 619 | 620 |
| 709 | 714 | 714 |
| 843* | | 833 |
| | 863 | |
| | | 875 |
| 893* | | |
| 1015 | 1026 | |
| | | 1043 |
| 1132 | | |
| | | 1165 |
| 1192 | 1199 | 1199 |
| | 1295 | 1257 |
| 1341 | 1342 | 1355 |
| 1400 | 1411 | |
| | | 1423 |
| | | 1434 |
| 1451 | 1448 | 1450 |
| 1520 | 1521 | 1526 |
| 1580 | 1568 | 1580 |
| | 1604 | 1613 |

At this point, we must notice that quantitatively reversed is the behaviour of 412 cm$^{-1}$ band, which is only barely seen in the fluorescence spectrum of PHN, although calculations do not predict any drastic change of its intensity as compared to the corresponding 408 cm$^{-1}$ band in the fluorescence spectrum of PH. According to our calculations, the displacement parameters $\Delta$ for 408 cm$^{-1}$ band in PH and for 412 cm$^{-1}$ band in PHN spectrum are 0.040 and 0.022, respectively (which is a rather moderate decrease). Furthermore, the 400 cm$^{-1}$ frequency range can be considered in the case of PHN, as the region of many close-lying fundamental vibrational modes. On the other hand, in the case of BQ a relevant vibrational mode (which is 410 cm$^{-1}$, cf. Table II and Fig. 3 in [2]) was found to undergo only minor change of its intensity. But the "effects" of both kinds (i.e. either "enhancement" or "quenching" of different vibrational bands) were also observed in the case of BQ molecule even though vibrational structure of its fluorescence spectrum was much better resolved.

In order to get some more insight in all the above-described similarities and differences between the fluorescence spectra of PH molecule and its both monoazaderivatives (PHN and BQ), we summarize our knowledge about the changes due to the substitution of N atom into the aromatic ring system of PH and those caused by electronic transition from $S_0$ ground state to $S_1$ excited state, in all three molecules under consideration (or in other words we will compare the ground and excited state equilibrium structures of these molecules).

### 3.3. The ground- and excited-state equilibrium (optimized) geometry of phenanthrene and monoazaplenathrenes

As was mentioned earlier in Sect. 2, substitution of an N atom into the PH molecule results in changes of the lengths of chemical bonds and the angles between adjacent bonds, and in the ground state of monoazaphenantrenes (either PHN or BQ) an aromatic rings system of parent PH molecule undergoes deformation (its $C_{2v}$ symmetry is broken or reduced to $C_s$ symmetry). It was also concluded that although the extent of deformation depends on the position of substitution of N atom, in both monoazaphenanthrenes deformation is not confined to the ring in which N atom resides but extends also over entire aromatic rings system [9].

Let us now inspect what happens when these molecules are excited to the $S_1$ electronic state. According to our discussion in Sect. 2, the differences between the optimized equilibrium geometry of the ground and excited singlet states of PHN molecule upon $S_0 \rightarrow S_1$ transition (expressed in Fig. 1 in terms of changes of the bonds lengths) are the largest in the central ring, where N atom is located, and smaller in the peripheral aromatic rings. It may look a bit surprising, but the same character of changes upon excitation was found earlier in the case of BQ molecule [7]. Although in this molecule N atom resides in the peripheral ring, the largest changes of the lengths of bonds, caused by transition to the excited state, are induced in the central ring (cf. Fig. 1 in [7]), and they are even larger than in PHN case. Furthermore, exactly the same pattern of changes is observed in PH

molecule (collected also in Fig. 1 of Ref. [7]), which as an aromatic molecule does not contain N atom at all. With such observations as above, one arrives at the conclusion that in all three molecules — both monoazaphenanthrenes as well as in their parent aromatic hydrocarbon — an electronic transition in the first excited singlet state is delocalized over entire aromatic rings system in very similar manner (which intuitively is not surprising, in view of the fact that in all three molecules $S_1$ state is of $\pi\pi^*$ character [5, 9]).

A complete information about the deformation of a given molecule caused by an electronic transition to its excited state, must also contain the changes of the angles between adjacent bonds. Only these two parameters together (i.e. changes of bonds lengths and changes of the values of angles between the bonds) describe the motion (direction and magnitude of the displacement) executed by individual atoms upon the transition from ground to excited state of the molecule. Table III collects calculated angles between different bonds in  the ground and excited state

TABLE III

Angles between adjacent chemical bonds in phenanthridine and 7,8-benzo-quinoline in the ground $\angle(S_0)$ and in the excited $\angle(S_1)$ state and their change between these states $\Delta(S_1-S_0)$. For the details of bond angles numeration see Fig. 4. Bold numbers are those corresponding to the N atom position in PHN and BQ.

| Angle no. | Phenanthridine | | | 7,8-benzoquinoline | | |
|---|---|---|---|---|---|---|
| | $\angle(S_0)^0$ | $\angle(S_1)^0$ | $\Delta\ (S_1-S_0)$ | $\angle(S_0)^0$ | $\angle(S_1)^0$ | $\Delta\ (S_1-S_0)$ |
| **1** | **118.54** | **118.98** | **0.42** | 121.14 | 121.82 | 0.68 |
| 2 | 124.69 | 124.92 | 0.23 | 120.85 | 121.31 | 0.46 |
| 6 | 123.09 | 122.84 | −0.25 | 119.69 | 118.49 | −1.19 |
| 3 | 118.42 | 117.96 | −0.46 | 119.80 | 118.98 | −0.82 |
| 5 | 117.86 | 117.65 | −0.21 | 119.12 | 120.02 | 0.90 |
| 4 | 117.40 | 117.67 | 0.27 | 119.41 | 119.38 | −0.03 |
| 13 | 120.62 | 121.30 | 0.68 | 120.61 | 121.39 | 0.78 |
| 8 | 120.34 | 120.93 | 0.59 | 119.52 | 119.45 | −0.07 |
| 14 | 119.94 | 119.04 | −0.90 | 119.28 | 119.23 | −0.05 |
| 7 | 120.56 | 119.81 | −0.75 | 117.75 | 117.56 | −0.19 |
| 18 | 119.80 | 120.05 | 0.25 | 120.05 | 119.53 | −0.52 |
| 9 | 119.40 | 118.81 | −0.59 | 117.98 | 118.49 | 0.51 |
| 17 | 120.30 | 120.47 | 0.17 | 120.32 | 121.02 | 0.70 |
| 10 | 120.98 | 120.86 | −0.12 | 123.72 | 124.57 | 0.85 |
| 16 | 121.01 | 121.47 | 0.46 | 120.43 | 121.04 | 0.61 |
| **11** | 120.56 | 121.20 | 0.64 | **118.98** | **118.69** | **−0.29** |
| 15 | 118.32 | 117.67 | −0.65 | 119.30 | 117.81 | −1.49 |
| 12 | 118.16 | 117.40 | −0.76 | 122.04 | 121.25 | −0.79 |
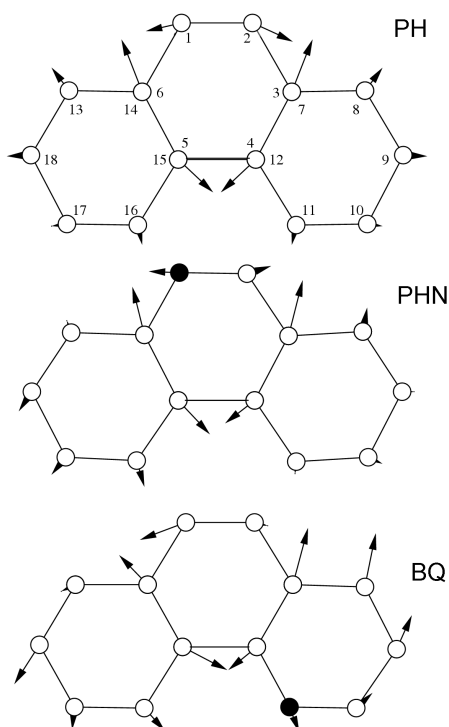
Fig. 4. Optimized equilibrium geometry of excited $S_1$ singlet state of PH, PHN, and BQ molecules (position of nitrogen atom in PHN and in BQ is marked by the black dot). The solid arrows attached to the atoms are the displacement vectors, which represent the direction of motion of a given atom and the magnitude of its displacement upon $S_0 \rightarrow S_1$ transition (their magnitude are not in scale with the molecular size and has been magnified by the factor of 30). Numbers (1–18) in PH structure define bond angles formed in all three molecules by adjacent chemical bonds (cf. Table III and the text).

for PHN and BQ molecule, and in Fig. 4 the motion executed by individual atoms upon excitation in all three molecules is illustrated.

Inspection of Fig. 4 shows that in the case of PH molecule, electronic transition to excited $S_1$ state does not change the ground-state symmetry of the molecule — from the point of view of the displacement vectors of all the atoms, symmetry of PH molecule does not change. This is also reflected by the changes of the angles between adjacent bonds (not given in Table III). The magnitudes of changes for pairs of adjacent bonds (with a common C atom) are the same after symmetry operations. For instance upon excitation of PH, the pairs of angles 1 and 2, 6 and 3, 17 and 10, 15 and 12, are changed by 0.56°, –0.86°, 0.58°, and –1.19°, respectively, and so on. These observations are in good agreement with a well-known fact [8, 14] that the symmetry of phenanthrene's ground and first excited singlet states is the same ($C_{2v}$).

Contrary to the case of PH molecule, the data of Fig. 4 and Table III reveal quite different situations in the case of both monoazaderivatives of PH. Neither the symmetry of motion executed by individual atoms nor the symmetry of changes of bond angles can be traced upon excitation of PHN and BQ molecules. It is very clear that the motion (or displacement) of atoms in the excited state (cf. Fig. 4) of both molecules results in the deformation of the tricyclic rings system, and this deformation is more pronounced in the case of peripheral rings of BQ molecule. Such a conclusion seems to be also confirmed by the difference of bond angles changes observed for PHN and BQ upon excitation. It is especially clearly seen when the bond angles 13 and 8, or 16 and 11, or 15 and 12 in peripheral rings, or 5 and 4 in the central ring of both molecules are compared (cf. Table III). These changes are not only appreciably different in their magnitudes (usually larger in the case of BQ) but they are also different in their signs (increase or decrease) in both molecules. As it was inferred earlier from the discussion of changes of the ground--state equilibrium geometry, which were caused by the substitution of N atom into the aromatic rings system of PH [9], also in the excited state, deformation of this aromatic rings system of PH is topologically more extended in the case of BQ molecule. It seems that these are the reasons of larger vibrational activity and richer vibrational structure observed in the fluorescence excitation and in the fluorescence (dispersed) spectra of BQ, as compared to spectra of either PHN (cf. Figs. 2 and 3 in [6]) or PH molecules.

## 4. Summary and concluding remarks

The analysis of laser induced single-vibronic-level fluorescence spectrum of jet-cooled phenanthridine molecule, carried out in this work, and the comparison of its results with the results of preceding analysis of the fluorescence spectrum of 7,8-benzoquinoline (observed under the same experimental conditions [6, 7]) has confirmed our earlier conclusions that similarities and differences between the vibrational structure of the spectra of both molecules can be understood and rationalized in terms of symmetry based arguments.

Introduction of N atom into the PH molecule results in reduction of its relatively high symmetry and in the deformation of either PHN or BQ molecules in the both, ground and excited singlet state. Low symmetry of both monoazaphenanthrenes is the main reason of increased vibrational activity in their fluorescence spectra (compared to PH fluorescence spectrum). Increased number of vibrations active in the electronic transition means that some of non-totally symmetric planar vibrations of phenanthrene may become active (in the Franck–Condon sense) in its monoazaderivatives and the vibronic structure of their fluorescence spectra becomes richer (compared to fluorescence spectrum of PH), which in fact is observed.

The observed order of increasing vibrational activity (which is: PH → PHN → BQ) agrees well with conclusion of the present analysis, according to which BQ

molecule suffers topologically more extended deformations (than PHN molecule) upon electronic transition to its first excited singlet state. On the other hand, in both monoazaphenanthrenes very distinct effect of mirror-symmetry breakdown between fluorescence excitation and dispersed fluorescence spectra can be observed. Thus, similarly to the case of PH molecule also in both monoazaphenanthrenes, mechanism of increased vibronic activity in $S_0 \rightarrow S_1$ and $S_1 \rightarrow S_0$ transitions cannot be related only to the geometry changes between both states, but presumably includes also other contributions of vibronically induced origin and/or due to the interference of Condon allowed and Herzberg–Teller induced transition moments. It seems, however, that vibronic coupling may be of particular importance in the case of BQ molecule in which $S_1$ state is described by strong configuration interaction of 4 excited configurations (including $n, \pi^*$ electronic configuration) which results in the oscillator strength, $f = 0.044$, for $S_0 \rightarrow S_1$ electronic transition [9] — and this is to be compared with corresponding values of 0.007 or 0.001 for PHN and PH molecules, respectively [9].

More detailed analysis of possible mechanisms of increased vibrational activity in the spectra of monoazaphenanthrenes, must await for a new set of experimental data, which would allow more precise determination of frequencies of vibrational modes and reliable determination of their intensities.

## Acknowledgments

## Note added in proof

While printing of this paper we have learned about recent publication [15] of mid-infrared ground-state spectra of phenanthridine in Ar matrix at 15 K (and also in solid H$_2$O). We notice an excellent agreement (in $740-3120$ cm$^{-1}$ range, available in publication [15]) between this spectrum and the data of [12] cited in Table II of present work. We want to thank Dr. M.P. Bernstein (of NASA Ames Research Center) for a fast response to our search for his paper.

## References

[1] R.S. Becker, *Theory and Interpretation of Fluorescence and Phosphorescence*, Wiley–Interscience, New York 1969.

[2] E.C. Lim, in: *Excited States*, Ed. E.C. Lim, Vol. 3, Academic Press, New York 1977, p. 305.

[3] L.A. Diverdi, M.R. Topp, *J. Phys. Chem.* **83**, 3477 (1984).

[4] J. Prochorow, I. Deperasińska, O. Morawski, *Chem. Phys. Lett.* **316**, 24 (2000).

[5] M. Norek, J. Dresner, J. Prochorow, *Acta Phys. Pol. A* **104**, 425 (2003).

[6] J. Prochorow, I. Deperasińska, Y. Stepanenko, *Chem. Phys. Lett.* **399**, 239 (2004).

[7] I. Deperasińska, J. Prochorow, Y. Stepanenko, *Acta Phys. Pol. A* **106**, 535 (2004).

[8] J.A. Warren, J.M. Hayes, G.J. Small, *Chem. Phys.* **102**, 323 (1986).

[9] I. Deperasińska, J. Prochorow, *Acta Phys. Pol. A* **104**, 601 (2003).

[10] Gaussian 98, Revision A.9, M.J. Frisch, G.W. Trucks, H.B. Schlegel, G.E. Scuseria, M.A. Robb, J.R. Cheeseman, V.G. Zakrzewski, J.A. Montgomery, Jr., R.E. Stratmann, J.C. Burant, S. Dapprich, J.M. Millam, A.D. Daniels, K.N. Kudin, M.C. Strain, O. Farkas, J. Tomasi, V. Barone, M. Cossi, R. Cammi, B. Mennucci, C. Pomelli, C. Adamo, S. Clifford, J. Ochterski, G.A. Petersson, P.Y. Ayala, Q. Cui, K. Morokuma, D.K. Malick, A.D. Rabuck, K. Raghavachari, J.B. Foresman, J. Cioslowski, J.V. Ortiz, A.G. Baboul, B.B. Stefanov, G. Liu, A. Liashenko, P. Piskorz, I. Komaromi, R. Gomperts, R.L. Martin, D.J. Fox, T. Keith, M.A. Al-Laham, C.Y. Peng, A. Nanayakkara, M. Challacombe, P.M.W. Gill, B. Johnson, W. Chen, M.W. Wong, J.L. Andres, C. Gonzalez, M. Head-Gordon, E. S. Replogle, J.A. Pople, Gaussian, Inc., Pittsburgh PA, 1998.

[11] A. Bérces, M.Z. Zgierski, in: *Computational Molecular Spectroscopy*, Eds. P. Jensen, P.R. Bunker, Wiley, Chichester 2000, p. 109.

[12] M.J. Nowak, to be published.

[13] P. Kolek, K. Pirowska, J. Najbar, *Phys. Chem. Chem. Phys.* **3**, 4874 (2001).

[14] G. Fischer, *Chem. Phys.* **4**, 62 (1974).

[15] M.P. Bernstein, A.L. Mattioda, S.A. Sanford, D.M. Hudgins, *ApJ* **626**, 909 (2005).